DOI: 10.1002/asia.200800083

Fullerene-like $Mo(W)_{1-x}Re_xS_2$ Nanoparticles

Francis Leonard Deepak,[a] Ronit Popovitz-Biro,[b] Yishay Feldman,[c] Hagai Cohen,[c] Andrey Enyashin,[d] Gotthard Seifert,[d] and Reshef Tenne*[a]

Dedicated to Professor Ryoji Noyori on the occasion of his 70th birthday

Abstract: Inorganic fullerene-like (IF) $Mo_{1-x}Re_xS_2$ and $W_{1-x}Re_xS_2$ nanoparticles have been synthesized by a gas-phase reaction involving the respective metal halides with H_2S. The IF-$Mo(W)_{1-x}Re_xS_2$ nanoparticles, containing up to 5% Re, were characterized by a variety of experimental techniques. Analyses of the X-ray powder diffraction and different electron microscopy techniques show that the Re is doped in the MoS_2 host lattice. Interestingly, Re-doped MoS_2 nanotubes are present as well, although in small quantities (~5%). XPS results confirm the nanoparticles to be more n-type arising from the effect of Re doping. Additionally, density-functional tight-binding (DFTB) calculations support the observed n-type behavior.

Keywords: density functional calculations · electron microscopy · fullerenes · nanotubes · rhenium

Introduction

MoS_2 and WS_2 are quasi two-dimensional (2D) compounds. Atoms within a layer are bound by strong covalent bonds, in which individual layers are held together by van der Waals (vdW) interactions. The stacking sequence of the layers can lead to the formation of either a hexagonal polymorph with two layers in the unit cell (2H); rhombohedral with three layers (3R) or a WTe_2-type structure.[1] The weak interlayer vdW interactions offer the possibility of introducing foreign atoms or molecules between the layers by intercalation.[2] Transition-metal dichalcogenide ReS_2 is a diamagnetic semiconductor that possesses an indirect gap in the near-infrared (NIR) region of about 1.37 eV. The layered structure ReS_2 is of considerable interest for various applications because of its optical, electrical, and mechanical properties. These applications include a sulfur-tolerant hydrogenation and hydrodesulfurization catalyst, and possibly also as a photoresponsive material in electrochemical solar cells.[3] The ReS_2 framework has the substructural motif consisting of Re_4-parallelogram units, which distort the lattice from the ubiquitous hexagonal motif of layered compounds. With respect to the bulk structure, this distortion results in a reduction of symmetry from $P6_3/mmc$ to $P\bar{1}$. With regards to the bonding properties, the d^3-Re center, which forms part of the t_{2g} band, has two electrons strongly hybridized with the p orbitals of sulfur. The remaining d electrons reside in the delocalized $d_{x^2-y^2}$ and d_{xy} metal orbitals. It is the overlap of these orbitals with neighboring Re centers that form the Re_4-parallelogram units containing Re−Re metal bonds. This, in turn, results in a gap in the middle of the bonding and antibonding-t_{2g} bands, thus giving rise to the semiconducting nature of ReS_2.[4] Nanoparticles of MoS_2, WS_2, ReS_2, and a plethora of other 2D compounds are known to form closed-cage structures, which are referred to as inorganic fullerene-like (IF) structures and inorganic nanotubes (INT), analogous to the respective nanostructures formed from carbon.[1] The first report on the use of the gas-phase reaction to prepare IF-NbS_2 nanoparticles is noticeable.[5] One of the early methods of synthesis of IF-MoS_2 and IF-WS_2, which is currently going through industrial scale-up, in-

[a] Dr. F. L. Deepak, Prof. Dr. R. Tenne
Department of Materials and Interfaces
Weizmann Institute of Science
Rehovot 76100 (Israel)
Fax: (+972) 89 344 138
E-mail: reshef.tenne@weizmann.ac.il

[b] Dr. R. Popovitz-Biro
Electron Microscopy Unit
Weizmann Institute of Science
Rehovot 76100 (Israel)

[c] Dr. Y. Feldman, Dr. H. Cohen
Chemical Research Support Unit
Weizmann Institute of Science
Rehovot 76100 (Israel)

[d] Dr. A. Enyashin, Prof. Dr. G. Seifert
Physical Chemistry
Technische Universität Dresden
01062 Dresden (Germany)

volved starting from the respective oxide nanoparticles.[6] Subsequently, synthesis using a gas-phase reaction starting from $MoCl_5/WCl_n$ and H_2S has been demonstrated.[7a,b] A similar strategy for the synthesis of IF-MoS_2 nanoparticles using the gas-phase reaction between $Mo(CO)_6$ and sulfur, has been reported as well.[7c] The two kinds of reactions progress along very different paths, which has a large effect on the topology of the closed-cage nanoparticles. The conversion of the metal-oxide nanoparticles to sulfides (IF) starts on the surface of the nanoparticles progressing gradually inwards in a slow diffusion-controlled fashion.[6d–f] Contrarily, the gas-phase reaction proceeds by a nucleation-and-growth mode starting from, for example, a small MoS_2 nuclei and progressing outwards rather rapidly.[7] IF-ReS_2 nanoparticles have been prepared by the direct sulfidization of ReO_2, formed from the decomposition of ReO_3.[8] By adopting the multiwalled carbon nanotube (MWCNT)-templating approach, it has also been possible to prepare nanotubes of ReS_2.[9]

Bulk single crystals of 0.5% and 1% rhenium-doped (Re-doped) $Mo(W)S_2$ have been grown by the chemical vapor transport method with Br_2 as a transport agent. The effect of Re doping has been determined to play a major role in influencing the electrical and optical properties of the doped samples.[10] Furthermore, a study of Mo-doped ReS_2 single crystals has shown that the incorporation of molybdenum into $ReSe_2$ has formed the specific impurity levels, which caused an increase of the electrical conductivity and a marked drop in the carrier mobility.[11] Thus, the doping of Re in $Mo(W)S_2$ induces n-type conductivity, which is the motivation for the present study.

The doping of inorganic fullerene-like (IF) nanoparticles and inorganic nanotubes (INT) is a subject of current interest. Doping of inorganic nanotubes has been reported for specific cases of Ti-doped MoS_2 nanotubes, Nb-doped WS_2 nanotubes, and Mo- and C-doped WS_2 nanotubes.[12a–d] W-alloyed MoS_2 nanotubes were synthesized by varying the W/Mo ratio.[12e–g] The effect of Nb substitution on the electronic structure of MoS_2 was investigated theoretically using density functional tight binding method (DFTB).[13] This work predicted that mixed $Mo_{1-x}Nb_xS_2$ nanotubes (with varying Nb contents) should exhibit a metallic character, independent of their chirality, diameters, and ordering type of the substitutional atoms. In effect, the density of states close to the Fermi level of the Nb-substituted MoS_2 tubes can be tuned over a wide range by the degree of Nb doping. This theoretical prediction was recently confirmed experimentally by doping (alloying) IF-MoS_2 nanoparticles with Nb.[14] The concentration of the Nb atoms in the MoS_2 lattice was as high as 30%. In this high Nb concentration, patches of the NbS_2 lattice are dispersed in the MoS_2 lattice forming a chessboard like 2D lattice within each layer. The Nb-doped (alloyed) IF-MoS_2 nanoparticles were thereby shown to be metallic. Doping of Nb in IF-MoS_2 induces p-type behavior, whereas in the present case, doping of Re would lead to n-type conductivity. Doping of IF and INT would encourage the idea for the application of Mo/WS_2 nanostructures in semiconducting nanoelectronic devices and as a conductive phase in nanocomposites with numerous potential applications. The band gap of MoS_2 nanotubes is similar to silicon: 0.89–1.07 eV, versus 1.17 eV for silicon. At the same time, S–Mo–S layers with coordinatively saturated surfaces are much more resistant against oxidation and humidity than silicon or other semiconductors of the groups IV, III–V, II–VI. Thus, the potential for applications of IF and INT could be considerably enlarged, because of a possibility of n- or p-type doping as for silicon.[1]

In the current study, mixed phase IF-$Mo(W)_{1-x}Re_xS_2$ nanoparticles are prepared by a vapor-based method starting from the respective volatile metal-chloride precursors in combination with H_2S. This method has been previously used for the successful synthesis of IF-MoS_2 and IF-WS_2 nanoparticles and nanotubes.[7a,b] The use of metal-chloride precursors to obtain IF-NbS_2, IF-TaS_2, and IF-TiS_2 nanoparticles by the vapor-phase reaction, albeit by different means, is well established.[5,15] One of the main advantages of this method, is that being a vapor-phase synthesis, it allows intimate mixing of the materials, namely Re, in this case with that of Mo/W.

Results and Discussion

IF-$Mo_{1-x}Re_xS_2$ Nanoparticles and Nanotubes

IF-$Mo_{1-x}Re_xS_2$ nanoparticles synthesized at 800 °C (Table 1, Series 1) resulted in both spherical and well-faceted nanoparticles of approximately 30 to 80 nm in diameter and interlayer spacing of approximately 0.62 nm. TEM-energy dispersive spectroscopy (EDS) and high resolution TEM-electron energy loss spectroscopy (EELS) analysis reveal the presence of Re in the nanoparticles.

The HRTEM images of the IF-$Mo_{1-x}Re_xS_2$ nanoparticles synthesized at 850 °C (Table 1, Series 2) are shown in Figure 1. The diameter of the IF-$Mo_{1-x}Re_xS_2$ nanoparticles is in the range of 50–80 nm. The EDS spectra of the IF-

Table 1. Details of the reactions carried out for the synthesis of the IF-$Mo_{1-x}Re_xS_2$ nanoparticle.

Temperature of the horizontal reactor	Temperature of the auxiliary furnace	Gas flow rates	Size of the IF-$Mo_{1-x}Re_xS_2$ nanoparticles
Series 1		Forming gas	30–80 nm
$T_1 = 800$ °C	$T_2 = 220$ °C	(I) = 50 cc (95%	
	$T_3 = 250$ °C	N_2 and 5% H_2)	
		H_2S (II) = 5 cc	
		N_2 (III) = 50 cc	
Series 2		Forming gas	50–80 nm
$T_1 = 850$ °C	$T_2 = 220$ °C	(I) = 50 cc (95%	
	$T_3 = 250$ °C	N_2 and 5% H_2)	
		H_2S (II) = 5 cc	
		N_2 (III) = 50 cc	
Series 3		Forming gas	50–100 nm IF-nanoparticles + nanotubes
$T_1 = 900$ °C	$T_2 = 220$ °C	(I) = 50 cc (95%	
	$T_3 = 250$ °C	N_2 and 5% H_2)	
		H_2S (II) = 5 cc	
		N_2 (III) = 50 cc	

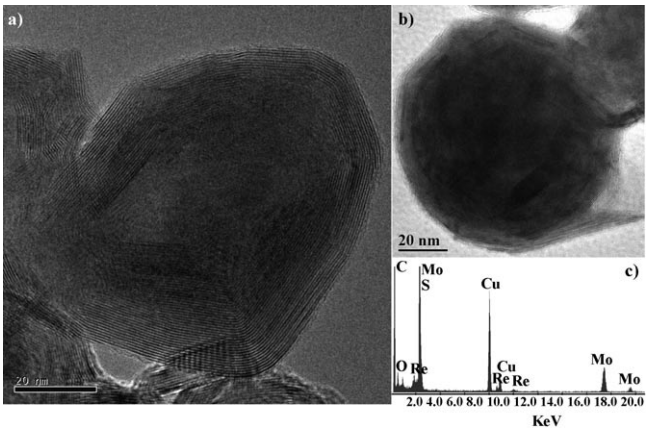

Figure 1. a) and b) HRTEM images of the IF-$Mo_{1-x}Re_xS_2$ nanoparticles synthesized at 850 °C. c) EDS spectra of the IF-$Mo_{1-x}Re_xS_2$ nanoparticle shown in (b).

$Mo_{1-x}Re_xS_2$ nanoparticle shown in Figure 1b is presented in Figure 1c. Rhenium atoms seem to be uniformly distributed in all the examined nanoparticles, irrespective of their size or shape. The presence of the characteristic and distinct Mo (K,L), S (K), and Re (M,L) lines can be clearly seen. From the TEM-EDS and the HRTEM-EELS analysis, the metal to sulfur ratio is determined to be 1:2. The stoichiometry of the IF-$Mo_{1-x}Re_xS_2$ nanoparticles is as follows: Mo/Re/S—0.97 (±0.01):0.03 (±0.01):2. Additional TEM-EDS and HRTEM-EELS analyses show that the Mo + Re/S ratio remained nearly constant, independent of the IF nanoparticle diameter and position.

Figure 2a shows a TEM image of a collection of the IF-$Mo_{1-x}Re_xS_2$ nanoparticles synthesized at 900 °C (Table 1, Series 3). Figure 2b shows the HRTEM image of a single nanoparticle. The diameter of the nanoparticles is between 50–100 nm at this temperature of synthesis. The presence of Re is ascertained from the EDS analysis carried out on individual as well as a collection of IF-$Mo_{1-x}Re_xS_2$ nanoparticles (Figure 2d). The presence of the characteristic and distinct Mo (K,L), S (K), and Re (M,L) lines can be clearly seen from the EDS spectra. Apart from obtaining IF-$Mo_{1-x}Re_xS_2$ nanoparticles, nanotubes of Re-doped MoS_2 were also obtained at 900 °C (Table 1, Series 3). The nanotubes come in small amounts (~5%). Figure 2c shows the HRTEM image of one such nanotube. The length of the nanotubes thus obtained is about half a micron, whereas the diameter is about ~40 nm (~25 layers). The interlayer spacing of the nanotube shown in Figure 2c is ~0.62 nm, which is very similar to that of pure IF-MoS_2.[6,7] The EELS spectra of the nanoparticles and nanotubes showed the characteristic Mo ($L_{3,2}$), S (K), and Re ($M_{4,5}$) signals, and the amount of Re in the particles was about 1–2 atomic percent. Higher temperatures of synthesis were found to be suitable for the production of the nanotubes. This observation was consistent with the synthesis of pure MoS_2 and WS_2 nanotubes, in which higher temperatures of synthesis (~900 °C) favored their formation.[7a,b]

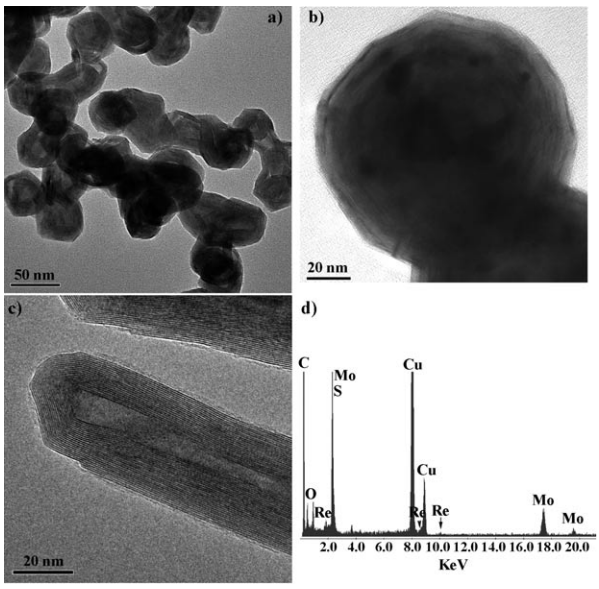

Figure 2. a) TEM image of a collection of IF-$Mo_{1-x}Re_xS_2$ nanoparticles synthesized at 900 °C. b) HRTEM image on one individual IF-$Mo_{1-x}Re_xS_2$ nanoparticle. c) HRTEM image of one individual Re-doped MoS_2 nanotube. d) EDS spectra of the IF-$Mo_{1-x}Re_xS_2$ nanoparticles.

Figures 3a and b show the XRD pattern of the IF-$Mo_{1-x}Re_xS_2$ nanoparticles synthesized at 850 °C (Table 1, Series 2,) and at 900 °C (Table 1 Series 3). The standard diffraction patterns of 2H-MoS_2, 2H-ReS_2 are also shown in the figure for comparison. It can be seen that all the peaks of the sample match well with those of 2H-MoS_2. The (002) peak in the XRD pattern was characterized by a shift to a lower angle as compared to the (002) peak in hexagonal 2H-MoS_2 crystals, indicating a small lattice expansion in the case of the IF nanoparticles and nanotubes.[6,7] This expansion has been attributed to the introduction of strain owing to curvature of the layers.[1,6,7] Comparison of the full width at half maximum of the (002) peaks (Figures 3a and b) confirm the TEM data that the size of the nanoparticles ob-

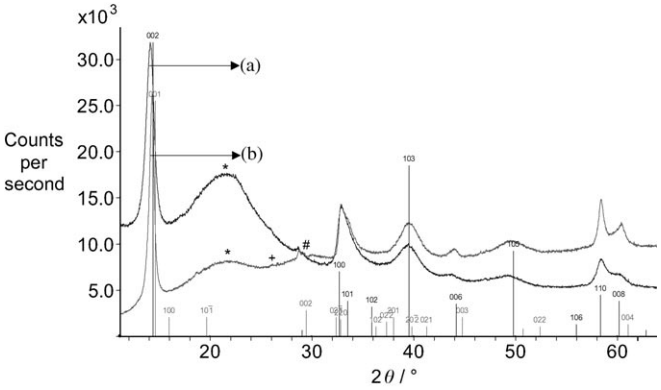

Figure 3. XRD pattern of IF-$Mo_{1-x}Re_xS_2$ nanoparticles prepared at (a) 850 °C and (b) 900 °C are shown. Standard diffraction patterns of 2H-MoS_2 and 2H-ReS_2 are also shown for comparison. The asterix in the diffraction pattern corresponds to the peak arising from the filter used for collecting the nanoparticles. The peak of the oxide of Re (ReO_3) (#) and Mo (MoO_2) (+) are shown.

tained at 900 °C is larger than those nanoparticles obtained at 850 °C. Any secondary phases of ReS_2 have been ruled out from the XRD pattern. However, the presence of a small proportion of ReO_3 and MoO_2 is present as can be seen in the figure. This is in accordance with the TEM observations, in which it is seen that the core of some of the nanoparticles reveal the presence of an oxide. Rhenium oxides have been found to be present in the core of the IF-ReS_2 nanoparticles synthesized previously.[8] However, the nature of the oxides found were complex and were found to be ReO_2 or amorphous ReO_x. In the present case, apart from the presence of ReO_3 (as revealed from XRD data), the possibility of ReO_2 (formed by disproportionation of ReO_3) or amorphous oxides of the type ReO_x cannot be conclusively ruled out. Of the various oxides, ReO_3 is known to resemble copper in appearance and exhibit good conductivity as well. Recently, ReO_3 nanoparticles (8.5–32.5 nm) were shown to be metallic.[16] ReO_2 is formed by disproportionation of ReO_3, resulting in the formation of both monoclinic and orthorhombic forms of the reduced oxide. These reduced forms were, in general, found to be more susceptible to sulfidization.[8]

Table 2 summarizes the XPS-derived atomic concentrations of the IF-$Mo_{1-x}Re_xS_2$ nanoparticles (Table 1, Series 3).

Table 2. XPS-derived compositions of the IF-$Mo_{1-x}Re_xS_2$ nanoparticles (Series 3, Table 1) given in atomic percentages.

Element	Atomic Concentration [%]
Re	0.02
Mo	2.98
S	5.78
O	37.55
C	28.50
Si	21.98

The characteristic Re (4f) signal is clearly seen along with that of Mo ($3d_{5/2}$) and S ($2p_{3/2}$) in the spectra, however, its quantity (~1 %) is of a relatively large uncertainty, arising from the neighboring Mo (3p) signal. The values in Table 2 are the average recorded over a number of experiments (10 experiments) and are in accordance with the atomic percentage of Re obtained with HRTEM-EELS.

The binding energies of Mo and S exhibit a marked difference when the Re-substituted and the unsubstituted IF samples are compared. This is clear evidence for the incorporation of Re into the Mo-based particles. The observed difference, is practically identical for the Mo and S lines, $\Delta = 200 \pm 100$ meV, and is verified to be beyond any possible charging effect. In these experiments, the charging conditions of the sample were changed systematically by varying the flux of the electron flood gun. Additionally, reference lines, like that of the gold substrate and the carbon contamination, do not show the relative shifts in the binding energy. It is concluded that the Δ shift arises from the Re incorporation into the lattice, which raises the E_F upwards, thus making the nanoparticles more n-type.

IF-$W_{1-x}Re_xS_2$ Nanoparticles

Shown in Figures 4a and b are the HRTEM images of IF-$W_{1-x}Re_xS_2$ nanoparticles synthesized at 900 °C (Table 3, Series 2). The diameter of the IF-$W_{1-x}Re_xS_2$ nanoparticles is found to be in between 50–75 nm in this set of experimental conditions. The nanoparticle in Figure 4a is well-elongated, whereas the nanoparticle in Figure 4b is clearly faceted. The interlayer spacing of the particle is found to be 0.62 nm as shown by the line profile in Figure 4a (inset). The similarity to the value of the interlayer spacing of pure IF-WS_2 suggests that here again the Re is present in lower percentages. The presence of Re is confirmed by the TEM-EDS analysis. Shown as an inset in Figure 4b is the EDS spectrum revealing the characteristic W (L,M), Re (L,M), and S (K) lines. The composition as ascertained from the TEM-EDS analysis is found to be as follows: W/Re/S—0.97 (±0.01):0.03 (±0.01):2.

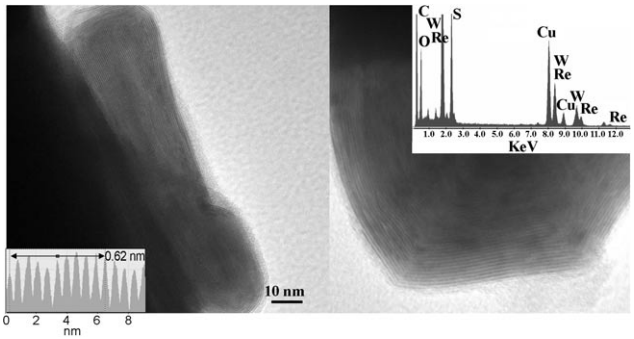

Figure 4. HRTEM images of the IF-$W_{1-x}Re_xS_2$ nanoparticles synthesized at 900 °C.

Table 3. Details of the reactions carried out for the synthesis of the IF-$W_{1-x}Re_xS_2$ nanoparticles.

Temperature of horizontal reactor	Temperature of auxiliary furnace	Gas flow rates	Size of the IF-$W_{1-x}Re_xS_2$ nanoparticles
Series-1		Forming gas	~100 nm
$T_1 = 850$ °C	$T_2 = 300$ °C	(I) = 100 cc (95 %	
	$T_3 = 325$ °C	N_2 and 5 % H_2)	
		H_2S (2) = 10 cc	
		N_2 (3) = 50 cc	
Series-2		Forming gas	50–75 nm
$T_1 = 900$ °C	$T_2 = 300$ °C	(I) = 100 cc (95 %	
	$T_3 = 325$ °C	N_2 and 5 % H_2)	
		H_2S (2) = 10 cc	
		N_2 (3) = 50 cc	

In this study, both XRD and HRTEM indicate that Re is present as a dopant in the lattice (for both MoS_2 and WS_2) and not as an intercalant since the presence of Re as an intercalant would result in an additional lattice expansion in the spacing of the (002) layers.[1,2,14,17]

Attempting to dope both IF-MoS_2 and IF-WS_2 to values higher than 5 %, was found to result in a segregation of secondary phases and nonuniformity of the sample. MoS_2 crys-

tallizes in 2H or 3R structure, whereas ReS_2 crystallizes in a distorted C6 structure.[10] Therefore, it is not expected that the two different lattices intermix at any ratio, and solid solutions of ReS_2 and MoS_2 would be miscible. Similar behavior was found in the case of the growth of Re-doped MoS_2 single crystals, in which a 5% or higher nominal doping of Re in MoS_2 prevented the growth of single crystals.[10] Furthermore, contrary to other layered MS_2 compounds (MoS_2 and WS_2), ReS_2 in its bulk form contains metal–metal bonded clusters (Re_4) and metal atoms that are octahedrally rather than trigonal prismatically coordinated with sulfur.[4] Previously, in the case of doping Nb in MoS_2, it was found that up to 25% Nb was incorporated in the lattice of MoS_2. This is, however, not surprising because NbS_2 crystallizes with the 2H or 3R-structure modification similar to MoS_2.[14] Doping was investigated theoretically for the first time in the case of Nb in MoS_2 nanotubes by Seifert et al.[13] This study showed that it was possible to incorporate up to 25% Nb in MoS_2 nanotubes. Experimentally, Nb-doped WS_2 nanotubes (yield 10%) have been obtained with up to 10% Nb doping.[12a,b] Another work involved doping Ti in MoS_2 nanotubes.[12c] In these works it has not been possible to obtain large yields of nanotubes exclusively by doping because of varied issues, such as difference in structure and bonding of the various transition-metal dichalcogenides in comparison to the dopants. This also seems to be true for the present case. This issue however needs to be examined in detail both experimentally and theoretically.

DFTB calculations on Re-doped MoS_2 nanotubes were also carried out. Supported by the experimental findings that suggest the Re doping to be a substitutional one, a single Re atom was placed on a Mo site in the periodic supercell of an armchair-MoS_2 nanotube (Figure 5). Thus, the interaction between Re atoms can be neglected. The calculations were performed for (14,14), (21,21), and (28,28) nanotubes. A supercell composing of 3 unit cells was chosen (see Figure 6). The DFTB approach, which was previously used to study the electronic structure of pure and Nb-alloyed MoS_2 nanotubes,[13] was employed in the current work. All the MoS_2 nanotubes considered here are semiconductors (see Figure 6a), in which the upper part of the valence band and the lower part of the conduction band are characterized by Mo 4d states. It was observed that a substitutional doping by a single Re atom changes the profile of the DOS only slightly. There is also practically no influence on the visible nanotube radius. However, one can see the separation of a level at the lower edge of the Mo 4d valence band, which has a significant Re 5d contribution (Figure 6b, 6c). At the same time, the Fermi level is shifted close to the

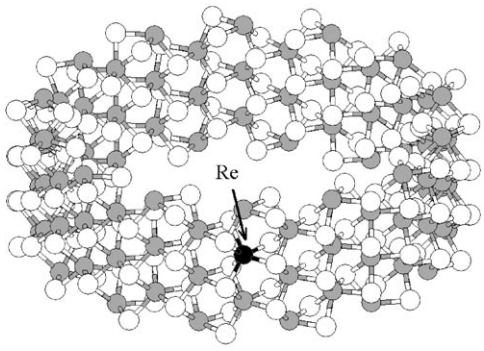

Figure 5. Structure of a fragment of Re-doped (14,14) MoS_2 nanotube.

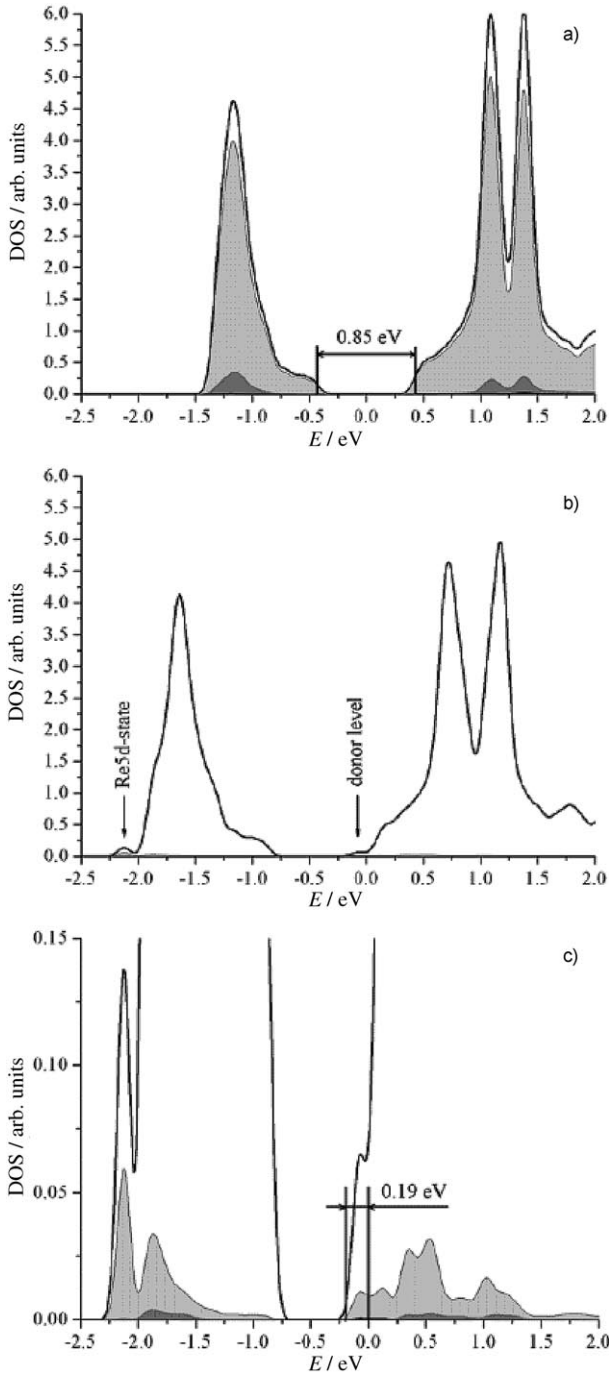

Figure 6. Densities of states (DOS) for a pure (14,14) MoS_2 nanotube (a) and for a Re-doped (14,14) $Mo_{1-x}Re_xS_2$ nanotube ($x = 1/84 \sim 1.2\%$) (b). Zoomed DOS profile of $Mo_{1-x}Re_xS_2$ nanotube is also shown (c). Mo 4d- and Re 5d-states are painted in gray in (a) and (b,c), respectively. Fermi level −0.0 eV.

lower edge of the conduction band. About 0.2 eV below the conduction band edge, a state with a considerable Re 5d character appears. This result is reminiscent of an n-type doping of a semiconductor. The replacement of the d^5s^1 Mo by the Re (d^5s^2) with one extra valence electron creates an occupied donor level just below the conduction band. The analysis of the charge distribution in this level shows that only about 20% can be attributed to Re 5d, whereas 80% are contributions from Mo 4d of the neighboring Mo atoms. The electrons in such a donor level are much more localized than in classical semiconductors, as for example, in the case of phosphorous-doped silicon. The range of this new state is only up to the second nearest Mo atom (~6 Å) with some trace to the next neighbor (~9 Å). There is no contribution from the electronic states of the S atoms. In a similar way, a p-type doping can be realized with a substitutional doping of Mo by Nb (d^4s^1) in the case of MoS_2.[18]

Conclusions

In summary, IF-$Mo(W)_{1-x}Re_xS_2$ nanoparticles and nanotubes with up to 5% Re have been obtained by the reaction of the respective metal halides with H_2S as the sulphidising agent. At lower temperatures, IF nanoparticles are obtained, whereas at higher temperatures, a small proportion of nanotubes (~5%) are obtained in addition to the nanoparticles. The Re atoms seem to occupy substitutional lattice sites in the host lattice. The Re doping of IF and INT of both MoS_2 and WS_2 constitute an important example of n-type doping of nanostructures. Further studies on the stability, electronic, and conduction properties of n- and p-doped Mo/WS_2 nanotubes, and fullerene-like nanoparticles by substitutional doping with Re and Nb are in progress.[18]

Experimental Section

Synthesis of IF-$Mo_{1-x}Re_xS_2$ Nanoparticles and Nanotubes

The synthesis of the IF-$Mo_{1-x}Re_xS_2$ nanoparticles was carried out as follows. The precursors for the synthesis of IF-$Mo_{1-x}Re_xS_2$ nanoparticles were $MoCl_5$ (m.p. = 194 °C; b.p. = 268 °C) and $ReCl_5$ m.p. = 220 °C. Initially, the precursors (Table 4) were heated in a separate auxiliary furnace and the vapors were carried into the main horizontal reactor.[19]. The $MoCl_5$ and $ReCl_5$ vapor, mixed along with the carrier gas and the H_2S gas (diluted with N_2), were provided from opposite directions of the reactor, respectively. This enables the reaction to occur in the central hot region of the furnace while the product is swept by the flow and collected onto the filter. The set-up used is shown in Figure 7. The $MoCl_5$ and $ReCl_5$ vapors were obtained by preheating the respective precursors in the auxiliary heating system (Figure 7b). The vapors were carried to the main horizontal reactor chamber (Figure 7a) by N_2 gas flow (50–200 cc min^{-1}). The temperature of the precursor source was kept usually between 220 and 250 °C in the case of the synthesis of the IF-$Mo_{1-x}Re_xS_2$, which is close to the boiling point of the chlorides. The preheating temperature was found to be the most significant factor, determining the amount of precursor supplied to the reaction. A small overpressure (1.1 bar) was maintained by using a gas trap filled with NaOH (5%) solution in the gas outlet of the reactor. The temperature of the reaction chamber, at which the precursor and H_2S mix and react, was varied in the range of 800–900 °C (Table 1). The resulting $Mo_{1-x}Re_xS_2$ powder was collected using a filter. The flow rate of H_2S (5–10 cc min^{-1}) was controlled by means of a TYLAN model FC260 mass-flow controller. The H_2S was diluted by mixing this gas with a stream of N_2 gas (50–200 cc min^{-1} in this reaction) using another flow controller.

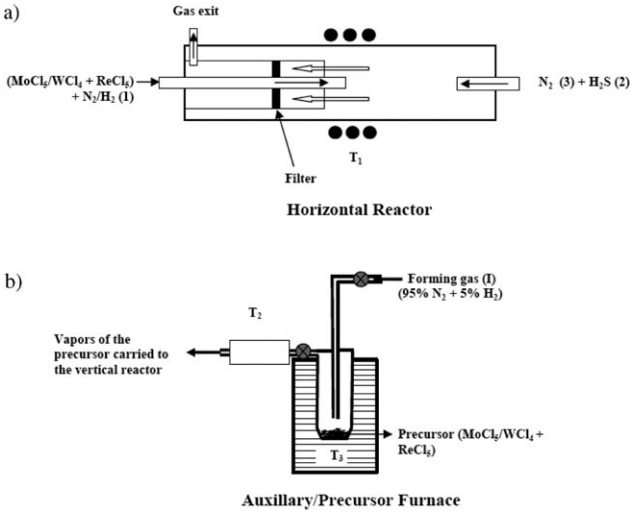

Figure 7. Two-stage furnace set-up employed for the synthesis of the IF-$Mo(W)_{1-x}Re_xS_2$ nanoparticles. a) Horizontal reactor and b) the secondary precursor heat furnace (auxiliary furnace).

Table 4. Details of the precursors used in the synthesis of the IF-$Mo_{1-x}Re_xS_2$ and IF-$W_{1-x}Re_xS_2$ nanoparticles.

Precursors	Melting point (m.p.)	Boiling point (b.p.)
Molybdenum Chloride ($MoCl_5$)	194 °C	268 °C
or	300 °C	–
Tungsten (IV) Chloride (WCl_4)		
Rhenium Chloride ($ReCl_5$)	220 °C	–

Synthesis of IF-$W_{1-x}Re_xS_2$ Nanoparticles and Nanotubes

The synthesis of the IF-$W_{1-x}Re_xS_2$ nanoparticles was carried out as follows: The precursors (Table 4) in this case of synthesis of the IF-$W_{1-x}Re_xS_2$ nanoparticles were WCl_4,(m.p.=300 °C and $ReCl_5$, m.p. = 220 °C. The flow rates of the various gases were maintained similar to the previous synthesis of the IF-$Mo_{1-x}Re_xS_2$ nanoparticles. The temperature of the reaction chamber (Figure 7a), at which the precursors and H_2S mix and react, was varied in the range of 800–900 °C (Table 2). The resulting $W_{1-x}Re_xS_2$ powder was collected using a filter.

Characterization

A vertical theta–theta diffractometer (TTRAX III, Rigaku, Japan) equipped with a rotating Cu anode operating at 50 kV and 200 mA was used for X-ray powder diffraction (XRD) studies. The measurements were carried out in the reflection Bragg–Brentano mode within the range of 10–70° of 2Θ-angles. XRD patterns were collected by a scintillation detector. The minute quantities of material available dictated a very slow data rate (0.05° min^{-1}). The peak positions and shapes of the Bragg reflections were determined by a self-consistent profile-fitting procedure using the Jade 8 software. XRD analysis was carried out on both the IF-$Mo(W)_{1-x}Re_xS_2$ (from this work) and IF-MoS_2/IF-WS_2 nanoparticles (used as a reference).[7a,b]

The following electron microscopes were used in this work: transmission electron microscope (Philips CM120 TEM) operating at 120 kV, equipped with EDS detector (EDAX-Phoenix Microanalyzer); and HRTEM with field emission gun (FEI Technai F30-UT) operating at 300 kV, equipped with a parallel electron energy loss spectrometer [Gatan imaging filter-GIF (Gatan)]. For electron microscopy and analysis, the collected powder was sonicated in ethanol and placed on a carbon-coated Cu grid (for TEM) or on lacy carbon-coated Cu grids (for HRTEM and EELS).

X-ray photoelectron spectroscopy (XPS) was carried out using a Kratos AXIS-HS spectrometer at a low power (75 W) of the monochromatized Al (Kα) source. The samples for XPS analyses were prepared by depositing a few drops of the nanoparticles sonicated in ethanol, onto an atomically flat Au substrate (SPI supplies, thickness—150 nm) or onto Au polycrystalline films coating on Si substrates.[14]

Acknowledgements

The support of the G. M. J. Schmidt Minerva center for Supramolecular architecture is acknowledged.

[1] a) R. Tenne, *Nat. Nanotechnol.* **2006**, *1*, 103; b) M. Remskar, *Adv. Mater.* **2004**, *16*, 1497.
[2] a) R. H. Friend, A. D. Yoffe, *Adv. Phys.* **1987**, *36*, 1; b) F. Levy, *Intercalated Layered Materials*, *Vol. 6*, Reidel, Dordrecht, **1979**.
[3] C.-H. Ho, *Opt. Express* **2005**, *13*, 9.
[4] a) H. H. Murray, S. P. Kelty, R. R. Chianelli C. S. Day, *Inorg. Chem.* **1994**, *33*, 4418; b) K. Friemelt, M.-Ch. Lux-Steiner, E. Bucher, *J. Appl. Phys.* **1993**, *74*, 5266.
[5] C. Schuffenhauer, R. Popovitz-Biro, R. Tenne, *J. Mater. Chem.* **2002**, *12*, 1587.
[6] a) R. Tenne, L. Margulis, M. Genut, G. Hodes, *Nature* **1992**, *360*, 444; b) L. Margulis, G. Salitra, R. Tenne, M. Talianker, *Nature* **1993**, *365*, 113; c) Y. Feldman, E. Wasserman, D. J. Srolovitz, R. Tenne, *Science* **1995**, *267*, 222; d) A. Zak, Y. Feldman, V. Alperovich, R. Rosentsveig, R. Tenne, *J. Am. Chem. Soc.* **2000**, *122*, 11108; e) Y. Feldman, G. L. Frey, M. Homyonfer, V. Lyakhovitskaya, L. Margulis, H. Cohen, G. Hodes, J. L. Hutchison, R. Tenne, *J. Am. Chem. Soc.* **1996**, *118*, 5362; f) Y. Feldman, V. Lyakhovitskaya, R. Tenne, *J. Am. Chem. Soc.* **1998**, *120*, 4176.
[7] a) F. L. Deepak, A. Margolin, I. Wiesel, M. Bar-Sadan, R. Popovitz-Biro, R. Tenne, *Nano* **2006**, *1*, 167; b) A. Margolin, F. L. Deepak, R. Popovitz-Biro, M. Bar-Sadan, Y. Feldman, R. Tenne, *Nanotechnology* **2008**, *19*, 095601; c) J. Etzkorn, H. A. Therese, F. Rocker, N. Zink, U. Kolb, W. Tremel, *Adv. Mater.* **2005**, *17*, 2372.
[8] K. S. Coleman, J. Sloan, N. A. Hanson, G. Brown, G. P. Clancy, M. Terrones, H. Terrones, M. L. H. Green, *J. Am. Chem. Soc.* **2002**, *124*, 11580.
[9] M. Brorson, T. W. Hansen, C. J. H. Jacobsen, *J. Am. Chem. Soc.* **2002**, *124*, 11582.
[10] a) K. K. Tiong, T. S. Shou, C. H. Ho, *J. Phys. Condens. Matter* **2000**, *12*, 3441; b) K. K. Tiong, P. C. Liao, C. H. Ho, Y. S. Huang, *J. Cryst. Growth* **1999**, *205*, 543; c) K. K. Tiong, T. S. Shou, *J. Phys. Condens. Matter* **2000**, *12*, 5043; d) K. K. Tiong, Y. S. Huang, C. H. Ho, *J. Alloys Compd.* **2001**, *317–318*, 208; e) P. C. Yen, Y. S. Huang, K. K. Tiong, *J. Phys. Condens. Matter* **2004**, *16*, 2171.
[11] a) P. C. Yen, M. J. Chen, Y. S. Huang, C. H. Ho, K. K. Tiong, *J. Phys. Condens. Matter* **2002**, *14*, 4737; b) S. Y. Hu, Y. Z. Chen, K. K. Tiong, Y. S. Huang, *Mater. Chem. Phys.* **2007**, *104*, 105.
[12] a) Y. Q. Zhu, W. K. Hsu, M. Terrones, S. Firth, N. Grobert, R. J. H. Clark, H. W. Kroto, D. R. M. Walton, *Chem. Commun.* **2001**, 121; b) Y. Q. Zhu, W. K. Hsu, M. Terrones, S. Firth, N. Grobert, R. J. H. Clark, H. W. Kroto, D. R. M. Walton, *Chem. Phys. Lett.* **2001**, *342*, 15; c) Y. Q. Zhu, W. K. Hsu, N. Yao, S. Firth, R. J. H. Clark, H. W. Kroto, D. R. M. Walton, *Adv. Funct. Mater.* **2001**, *11*, 69; d) Y. Q. Zhu, W. K. Hsu, C. B. Bothroyd, I. Kinloch, S. Trasobares, H. Terrones, N. Grobert, M. Terrones, R. Escudero, G. Z. Chen, C. Colliex, A. H. Windle, D. H. Fray, H. W. Kroto, D. R. M. Walton, *Chem. Mater.* **2000**, *12*, 3541; e) M. Nath, K. Mukhopadhyay, C. N. R. Rao, *Chem. Phys. Lett.* **2002**, *352*, 163; f) C. N. R. Rao, M. Nath, *Dalton Trans.* **2004**, 1; g) R. Tenne, C. N. R. Rao, *Philos. Trans. R. Soc. London Ser. A* **2004**, *362*, 2099.
[13] a) V. V. Ivanovskaya, T. Heine, S. Gemming, G. Seifert, *Phys. Status Solidi B* **2006**, *243*, 1757; b) V. V. Ivanovskaya, G. Seifert, A. L. Ivanovskii, *Russ. J. Inorg. Chem.* **2006**, *51*, 320.
[14] F. L. Deepak, H. Cohen, S. Cohen, Y. Feldman, R. Popovitz-Biro, D. Azulay, O. Millo, R. Tenne, *J. Am. Chem. Soc.* **2007**, *129* 12549.
[15] a) C. Schuffenhauer, B. A. Parkinson, N. Y. Jin-Phillipp, L. Joly-Pottuz, J. M. Martin, R. Popovitz-Biro, R. Tenne, *Small* **2005**, *1*, 1100; b) A. Margolin, R. Popovitz-Biro, A. Albu-Yaron, L. Rapoport, R. Tenne, *Chem. Phys. Lett.* **2005**, *411*, 162; c) A. Margolin, R. Popovitz-Biro, A. Albu-Yaron, A. Moshkovich, L. Rapoport, R. Tenne, *Curr. Nanosci.* **2005**, *1*, 253.
[16] K. Biswas, C. N. R. Rao, *J. Phys. Chem. B* **2006**, *110*, 842.
[17] A. Zak, Y. Feldman, V. Lyakhovitskaya, G. Leitus, R. Popovitz-Biro, E. Wachtel, H. Cohen, S. Reich, R. Tenne, *J. Am. Chem. Soc.* **2002**, *124*, 4747.
[18] A. N. Enyashin, G. Seifert, to be published.
[19] L. Song, L. Ci, L. Lu, Z. Zhou, X. Yan, D. Liu, H. Yuan, Y. Gao, J. Wang, L. Liu, X. Zhao, Z. Zhang, X. Dou, W. Zhou, G. Wang, C. Wang, S. Xie, *Adv. Mater.* **2004**, *16*, 1529–1534.

Received: March 10, 2008
Published online: July 4, 2008

